APPROXIMATING PDFS FOR MULTIPHASE FLOWS USING THE MAXIMUM ENTROPY METHOD

Stephen Scott[1], John Shrimpton[2], Graham Wigley[3]

1: Department of Mechanical Engineering, Imperial College London, stephen.scott@imperial.ac.uk
2: Department of Mechanical Engineering, Imperial College London, j.shrimpton@imperial.ac.uk
3: Department of Aeronautical and Automotive Engineering, Loughborough University, g.wigley@lboro.ac.uk

ABSTRACT

This paper assesses the suitability of the Maximum Entropy Method (MEM) for reconstructing multivariate multiphase flow PDFs (size and velocity). For this purpose PDA data for two different sprays (electrostatic and pressure swirl) have been used to generate PDFs and to obtain statistical integer moment constraints for the MEM. The resulting MEM based PDFs are compared with the original PDA based PDFs to assess the level and type of constraint necessary to achieve a reasonable approximation to the original data. Comparison shows that the required number of constraints is dependent on the complexity of the PDA PDF being reconstructed. As expected, simple Gauss like behaviour can be reproduced using just mean and variance constraints for the MEM. For more complex distributions it is necessary to constraint the MEM with higher order moments such as third order and covariance constraints.

1   INTRODUCTION

1.1   Background

Dispersed multiphase flows describe a large range of flow types from small scale injection sprays (e.g. in Diesel engines), to pollutant transport in large scale environmental systems. These flows are generally highly complex, e.g. a typical Diesel injection spray may contain millions of particles in any one realisation. This (solid or liquid) population may be polysized and can interact with one another (wake interactions, collisions, coalescence, breakup) and with the carrier phase over a large range of length and time scales. The carrier phase is normally turbulent in nature and this modifies the dynamic evolution of the dispersed phase particle population. Clearly the high dimensionality and complexity of these phenomena presents many challenges to engineers attempting to predict such flows computationally.

In principal it is possible to model polydispersed two phase flows using DNS (direct numerical simulation) if appropriate boundary, initial and interface conditions are selected to completely describe the physical situation. If such an approach was adopted the carrier phase would be modelled using the conventional Navier Stokes equations and the discrete particles could be modelled as moving boundaries. The force on each particle would be calculated as the surface integral of the fluid stress tensor. However, this is not feasible in practical high Reynolds number flows or in cases of inhomogeneous turbulence due to restrictions in computational resources. For this reason a number of methods have been developed to model such flows, each varying in underlying assumptions, levels of approximation and range of regime validity. Traditionally these methods have been grouped into two families - Lagrangian and Eulerian methods (see [1]). Lagrangian methods include direct numerical simulation (DNS with Lagrangian particle tracking), large eddy simulation (LES with Lagrangian particle tracking) and stochastic modelling (SM). Eulerian methods encompass Reynolds averaged Navier Stokes methods (RANS) and probability density function methods (PDF). These techniques can be alternatively classified as microscopic, mesoscopic or macroscopic according to the levels of approximation upon which the methods are based.

1. Microscopic methods attempt to model the full range of length and time scales present in the flow. Direct numerical simulation (DNS) is a prime example of a microscopic method. DNS is capable of resolving flow features of the Kolmogorov scale. The drawback of these methods is that they are computationally expensive and are hence limited to flows of relatively low Reynolds number.

2. Mesoscopic methods are, as the name suggests, a middle ground between microscopic and macroscopic methods. Large eddy simulation (LES) is a mesoscopic approach as the microscopic length and time scales are filtered out and modelled as a sub-grid model. Larger eddy transient features are resolved. These methods are more efficient than microscopic methods but are still computationally expensive.

3. Macroscopic methods involve only ensemble averaged quantities and consequently detailed flow structures cannot be reproduced. All turbulence features are modelled using a suitable turbulence model, such as the established

$k - \epsilon$ model. Reynolds averaged Navier Stokes (RANS) models are the most common of these methods and are commonly implemented in commercial CFD codes. Macroscopic methods are computationally efficient in comparison with DNS and LES.

Lagrangian methods involve solving the equations of motion and energy of the dispersed phase in a Lagrangian frame of reference, whereas the carrier phase equations are solved using a Eulerian framework. Due to the stochastic nature of the Lagrangian particle modelling method, large computation times are required because it is necessary to obtain representative ensemble of realisations in order to obtain statistically valid solutions. Additional problems are encountered with decreasing particle size such as the decreasing time-step needed to solve the particle equation of motion.

Until recently the Eulerian methods were dominated by the RANS or two-fluid approach in which a set of continuum equations representing conservation of mass, momentum and energy are derived for each phase. These models were derived using methods developed for single-phase turbulence modelling, such as the $k - \epsilon$ model. The equations are obtained by averaging the particle instantaneous equations over all realisations. This results in a closure problem that was normally resolved by appealing to empirical reasoning, once again established firstly for single-phase turbulence modelling. In the case of polysized dispersed particulate flows, the particle size distribution can be discretised into size 'bins' and Eulerian continuum equations can be written for each size class with appropriate exchange terms. This has the obvious effect of increasing the computation requirements.

More recently an alternative modelling method based on a kinetic approach has received increased attention. In this approach the continuum equations are derived from a transport equation for the probability density function (PDF) in particle phase space ([2, 3, 4]). The principal advantage in this approach is that the introduction of the PDF enables the transition from a stochastic description of individual particles within the flow, to the statistical ensemble of the particle ensemble as a whole. Mathematical closures for PDF techniques are often difficult to obtain and feasible to only a limited range of flow regimes.

1.2 Moment Transport Models

It is common in RANS methods to 'bin' the particle size range and transport each bin as an interpenetrating phase. Several authors have proposed dispersed phase transport models that involve transportation of moments of the particle size distribution ([5, 6]). This technique is broadly known as a 'moment transport model'. Moment transport models attempt to model polydispersed flows by transporting statistical moments of the particle distribution (size, velocity etc.) through physical space. By transporting moments it is possible to reconstruct approximate PDFs of the size distribution and from these other useful quantities may be calculated such as ensemble drag force. Moment methods have a number of closure issues which are analogous to those found in Reynolds stress modelling of single phase turbulence.

If a statistical description is adopted for multiphase flows then the phase space variables that characterise the flow are associated with probability distribution functions (PDFs) at any particular point in space and time. For example, the ith particle of the dispersed phase can be described in terms of particle velocity $\boldsymbol{U}^i$, position $\boldsymbol{X}^i$ and particle diameter Φ^i with corresponding phase space variables $\boldsymbol{u}$, $\boldsymbol{x}$ and ϕ. The (Klimontovich) fine grained phase space density function corresponding to these variables is then given as

$$f = \sum_i^N \delta[\boldsymbol{x} - \boldsymbol{X}^i]\delta[\boldsymbol{u} - \boldsymbol{U}^i]\delta[\phi - \Phi^i]. \tag{1}$$

Ensemble averaging of this density function over all realisations results in the definition of the probability density function.

Using the definition of the PDF and the Lagrangian equations for the trajectories of the particle properties, it is possible to derive a transport equation (e.g. using the Liouville theorem) for the particle PDF through phase space. This is analogous to the derivation of the Boltzmann equation from gas kinetic theory. From the PDF equation one can either compute the evolution of the PDF directly through phase space or derive transport equations for moments of the PDF which represent measurable statistical quantities. For the phase space variables we have selected above, the first technique requires simulation in a seven dimensional phase space domain in addition to time. The second method is analogous to the RANS (Reynolds averaged Navier Stokes) equations for turbulence modelling and is accompanied by the familiar problem of unclosed terms that require some form of modelling. In particular the need to provide estimates of higher order moments that need not necessarily have integer exponents.

The requirement of flexible closure methods for the second method is of interest in this paper. In many situations it is necessary to calculate acceleration terms (due to particle drag) and higher order correlations (e.g. triple order velocity fluctuations). In traditional approaches this information has been inferred from the available statistical information as found in the RANS technique. To model these unknown terms it would be advantageous to calculate or approximate the form of the multivariate PDF given the values of the transported moments. However, according to statistical theory there exist an infinite number of PDFs that correspond to a finite set of moments and additional information is necessary to

generate the PDF. Thus far, two approaches have been used in the literature to obtain the form of the particle size PDF only.

1. Use of a prescribed distribution such as Guassian or modified Rosin-Rammler distribution. This approach only considers the PDF of particle size and neglects velocity ([5]).

2. Use of the 'maximum entropy method' (MEM) which postulates that the form of the PDF can be determined if it is assumed that the PDF containing maximum 'information entropy' is the appropriate one to choose. MEM is not restricted to PDFs of size only, but can be extended to an arbitrary number of dimensions ([7]).

It is the maximum entropy method and it's suitability to closure methods in particulate flows that is of interest in this paper. The background to MEM is discussed in the following section.

1.3   Entropy Closures

When a moment approach is adopted to solving the phase space transport equation, problems are encountered because the governing equations for the Mth moment also depends on the $(M + 1)^{th}$ moment. This closure problem requires that we must infer information about higher order moments using the information we have available from the lower order moments. Archambault [7] recognised that this is similar to the moment problem found in the field of statistics where according to statistical theory, if we have a PDF p, of the variable x it is possible to obtain a unique reconstruction of the function only if we have an infinite number of moments of the general form

$$\int\limits_{-\infty}^{\infty} x^k p(x) \, dx = \langle x^k \rangle. \tag{2}$$

However, in practice only a finite number of moments are typically available (say, M) and under these conditions there exists an infinite number of distributions whose M moments coincide. No unique distribution exists for a finite number of moments.

When only a finite number of moments are available (as is normally the case) it is necessary to make at least one additional assumption in order to obtain a unique form of the distribution function. Archambault employed the maximum entropy (ME) method which is a technique first developed by Jaynes [8] based of the concept of statistical entropy which was previously proposed by Shannon [9]. According to Shannon, the (Shannon) entropy of a discrete distribution, p_i, is given as

$$S = -\sum_i p_i \ln p_i, \tag{3}$$

with the normalisation constraint and moment constraints given as

$$\sum_i p_i = 1, \text{ and } \langle A_r \rangle = \sum_i p_i A_{ri}, \quad r = 1, \ldots, M, \tag{4}$$

where A_r is a polynomial function of the phase space variables and M is the number of constraints. The ME method is equivalent to selecting the PDF of least bias, given the specified moment constraints. By choosing to use the ME distribution we are making the least possible assumptions regarding the statistical bias of the flow. Paris and Vencovska [10] provide a mathematical defence of the ME inference process and argue that the MEM is the only inference process respecting 'common sense'. The more moments we have available to constrain our PDF, the closer the PDF will be to the 'real' distribution.

The maximum entropy inference method has been applied in the field of atomisation, principally by Sellens [11] who pioneered the use of MEM to predict static drop size distributions in atomisers. Babinsky and Sojka [12] provide a summary of the techniques used for predicting drop size distributions and give a useful comparison between MEM and alternative methods. Triaballier *et al* [13] apply the maximum entropy formalism to liquid atomization problems to obtain a mathematical volume based drop-size distribution. In their work they show that this size distribution is capable of representing bimodal (two peaks) drop-size distributions. Volpe [14] investigates PDFs generated by MEM with a view to potential fluid dynamics applications. The work discusses properties of these PDFs and presents a 'small perturbation method' to obtain analytical closure relations for these PDFs (ie no need to solve for Lagrange parameters numerically).

1.4 Scope

If the maximum entropy method is to be successfully implemented in spray simulations it is essential that it can reasonable reproduce the dominant features of 'real' spray dynamics and transport. This paper examines the application of the MEM technique to reproduce PDFs for characteristic positions in two sprays. Phase doppler anemometry (PDA) data sets from a steady electrostatically charged kerosene spray and transient spray from a pressure swirl injector commonly used in direct injection spark ignition engines have been processed to obtain statistical moments of the spray PDFs. These moments have been used to constrain the MEM in an attempt to assess the suitability of the MEM and which moments are required to reproduce the PDFs to a sufficient level of accuracy. Firstly the PDA data is presented in the following section and then the MEM approach is discussed. Finally the results of the MEM analysis are presented and discussed with reference to the original PDA data.

2 PDA DATA

2.1 General

Two sprays are considered in this paper. The first spray is a transient spray produced using a pressure swirl atomiser [15] for use in direct ignition spark ignition (DISI) engines. The second spray was a steady state electrostatically charged kerosene spray [16]. Details of each spray and the locations considered will be presented in the following sections. The spray datasets were obtained using the phase doppler anemometry (PDA) method, measuring droplet size ϕ and two components of droplet velocity (axial u_z and radial u_r) simultaneously .

Contour plots for the PDFs were generated using a uniform cartesian orthogonal mesh in the droplet phase space. This presents a problem when determining the resolution of the grid to minimise the error within each bin, but preserving the shape of the PDF. This issue is demonstrated in Figure 1 which illustrates PDFs for a randomly generated multivariate gaussian dataset of $10,000$ points plotted using three different bin resolutions. Given that we know exactly how the marginal PDFs should look for a given set of parameters (means μ and variances σ^2), Figure 1 can be used to determine an appropriate number of data points per bin (approximately) according to the ratio N/n_b^2 where N is the total number of points in the dataset (10,000 in the case of Figure 1) and where n_b is the number of bin in each phase space dimension. The first set of PDFs show a low level of detail whereas the last set resolves random fluctuations in the distribution caused by the limited sample size. For the case of this simple Gaussian distribution a value of $N/n_b^2 = 25$ (Figure 1(b)) was deemed appropriate and this value was used as a guide for use in plotting PDFs for the spray datasets due to their similarity with the Gaussian distribution. Figure 1 also illustrates the increase in PDF peak values as the bin size is reduced which is an additional factor for consideration when comparing the MEM results with the original PDA data.

The raw datasets were used to calculate the moments of the droplet size and velocity PDF according to Equation 5. Both raw $\langle \phi^a u_z^b u_y^c \rangle$, and central $\mu_{a,b,c}$ moments were calculated where a, b and c are the moment indices.

$$\langle \phi^a u_z^b u_r^c \rangle = \frac{1}{N} \sum_{i=1}^{N} \phi_i^a u_{z,i}^b u_{r,i}^c \quad \text{and} \quad \mu_{a,b,c} = \langle (\phi_i - \langle \phi \rangle)^a (u_{z,i} - \langle u_z \rangle)^b (u_{r,i} - \langle u_y \rangle)^c \rangle \tag{5}$$

2.2 Spray Positions Considered

For the purposes of this paper three test cases are considered; two points in the transient DISI pressure swirl spray ($z = 20mm$, $r = 0mm$ and $z = 20mm$, $r = 7.5mm$) and one point in the steady charged spray ($z = 150mm$, $r = 0mm$). These points have been selected to highlight particular features of the maximum entropy method that will be discussed in the following sections.

The first spray was generated using a DISI pressure swirl injector spraying at 50 bar gasoline pressure into air under atmospheric conditions for a relatively long injection event of $5ms$. For the purposes of this investigation it was necessary to obtain pseudo-steady data from the transient history of the spray PDF at the positions chosen. To achieve this the transient data was processed into time bins or duration $0.1ms$ to identify a pseudo steady region as shown in Figure 2. PDA data points outside this pseudo-steady region were discarded ($t_{min} = 2ms$, $t_{max} = 5.0ms$). This lead to a 45% reduction in the dataset size. In addition to this the variance within each bin was calculated and checked for steady properties within this time interval.

The first position in the pressure swirl spray is axially located at a distance $z = 20mm$ from the injector. Figure 3 shows PDFs for this position in both the unfiltered (a) and filtered (b) states. This figure clearly shows that the filtering process has the effect of 'cleaning up' the shape of the PDFs by removing drops at the extremes of the size and velocity ranges. All three PDFs in this figure exhibit isotropy.

The second position in the pressure swirl spray is also at an axial distance of $z = 20mm$ in the spray at a radial distance of $r = 7.5mm$ which corresponds to a position in the edge of the spray plume. Figure 4 shows the PDFs for this position and in particular it highlights the correlation between axial and radial velocities.
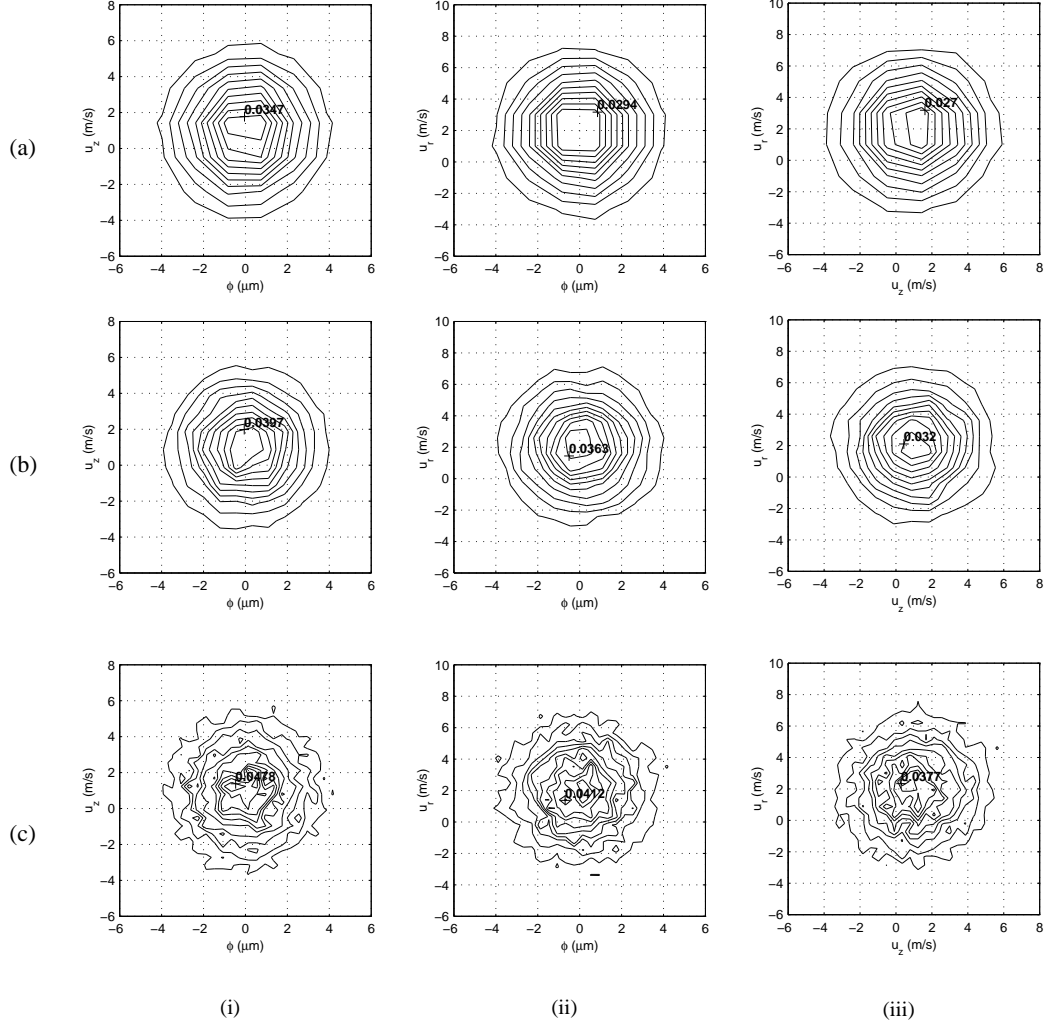
Figure 1: PDFs of (i) droplet size and axial velocity (ii) droplet size and radial velocity and (ii) axial velocity and radial velocity generated using random Gaussian number generator ($\mu_\phi = 0$, $\mu_{u_z} = 1$, $\mu_{u_r} = 2$, $\sigma^2_\phi = 3$, $\sigma^2_{u_z} = 4$, $\sigma^2_{u_r} = 5$). Plotted for (a) $N/n_b^2 = 100$ (b) $N/n_b^2 = 25$ (c) $N/n_b^2 = 6.25$.

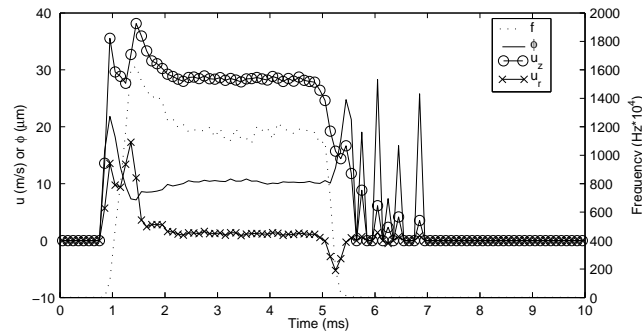Figure 2: PDA sample rate and mean quantities for DISI pressure swirl spray position 1 ($z = 20mm$, $r = 0mm$). PDA data sorted using $0.1ms$ bin size.

The second spray investigated is the steady charged hydrocarbon spray. The spray was produced using an atomiser with orifice diameter of $250\mu m$ and a flow rate of $1.67ml/s$ to give a mean injection velocity of $34m/s$ ($Re = 5100$ based on orifice diameter). The spray specific charge magnitude was $1.80C/m^3$ (see [16] for details). A single location in this spray is considered at a position of $z = 150mm$ and $r = 0mm$. Figure 5 shows PDF contour plots for this position. Of particular interest is Figure 5(i) which shows the non-linear drag relationship between droplet size and axial velocity,
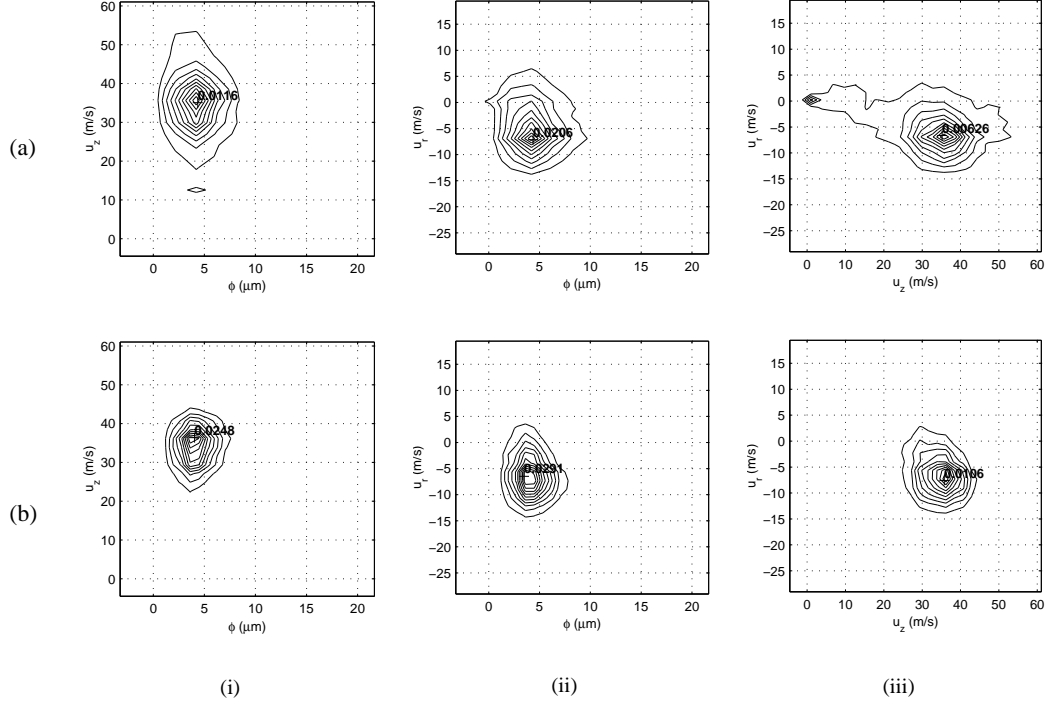
Figure 3: Unfiltered (a) and filtered (b) PDFs for the DISI pressure swirl spray position 1 ($z = 20mm$, $r = 0mm$). (i) Droplet size and axial velocity (ii) droplet size and radial velocity and (iii) axial velocity and radial velocity. Plotted using 30 by 30 grid ($N/n_b^2 \approx 25$).

Figure 4: Filtered PDFs for the DISI pressure swirl spray position 2 ($z = 20mm$, $r = 7.5mm$). (i) Droplet size and axial velocity (ii) droplet size and radial velocity and (iii) axial velocity and radial velocity. Plotted using 37 by 37 grid ($N/n_b^2 \approx 25$).

absent in Figures 3(b) and 4. The reason for the difference in the much larger range of diameters present in Figure 5 and the inertia these larger drops retain.

3   MEM IMPLEMENTATION

The solution of maximum entropy problem can be achieved using the method of Lagrange multipliers, λ, however this direct calculation requires the solution of a set of implicit non-linear equations. For problems of several phase-space dimensions with multiple constraints, solutions can be difficult to achieve and computationally expensive. An alternative to this method is to formulate a variational solution using the Lagrange multipliers as variational parameters according to the method of [17]. This method requires formulation of a single valued function F, according to domain and constraints, which itself is a function of the Lagrange parameters.

(i)   (ii)   (iii)

Figure 5: PDFs for the steady charged spray ($z = 150mm$, $r = 0mm$). (i) Droplet size and axial velocity (ii) droplet size and radial velocity and (iii) axial velocity and radial velocity. Plotted using 20 by 20 grid ($N/n_b^2 \approx 25$).
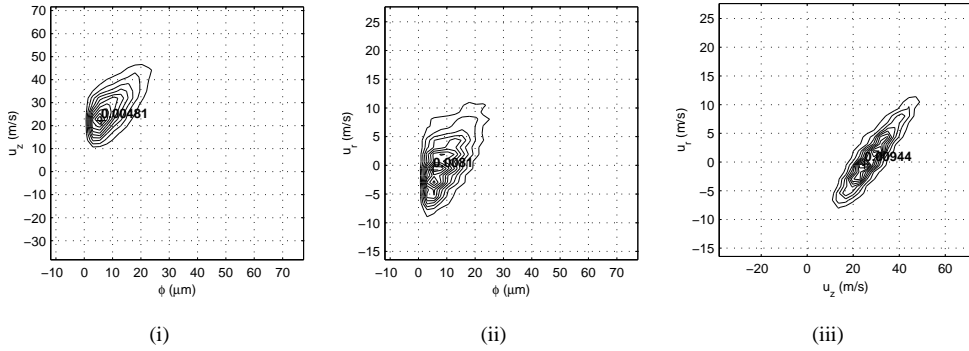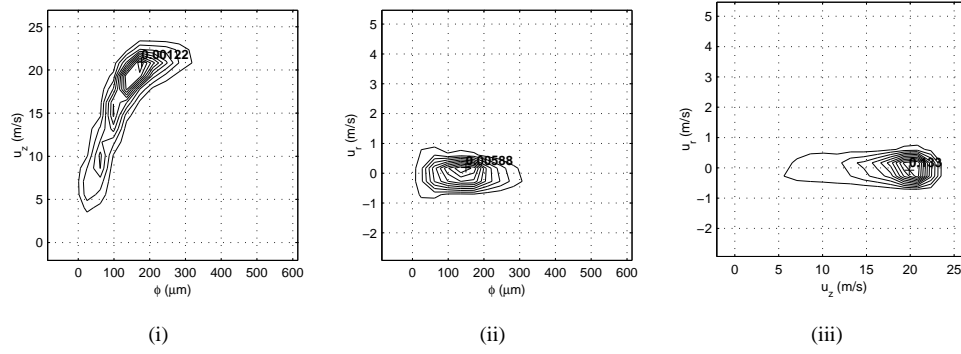
$$F = \ln \sum_i^N \exp \left(\sum_{r=1}^M -\lambda_r B_{r,i} \right) \quad \text{where} \quad B_{r,i} = A_{r,i} - b_r \tag{6}$$

To achieve maximum entropy this function must be minimised by varying λ. The calculated values of λ are used to generate the MEM PDF using Equation 7.

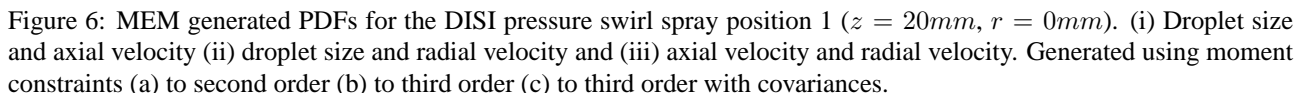$$p_i = \exp \left(-\lambda_0 - \sum_{r=1}^M \lambda_r A_{r,i} \right) \tag{7}$$

Computational speed was not of interest in this preliminary investigation, so for convenience the MEM was coded using MATLAB. Minimisation of Equation 6 was achieved using the Nelder Mead simplex minimisation algorithm [18]. The MEM code was tested by generating a multi-dimensional PDF using a Gaussian random number generator, taking the moments of this distribution, using these moments as constraints in the MEM code and comparing the results. Good correlations between distributions was achieved. The peak values of the test distributions was found to be sensitive to the grid selected for the MEM domain. As the grid is refined the peak value increases towards a maximum. It is believed that this is a resolution issue because at low resolutions the peak is not adequately resolved. Further investigation using the test distribution has indicated that a 40 by 40 domain is sufficient to resolve the peak correctly.

4   RESULTS AND DISCUSSION

In this section we present selected MEM generated PDFs using various different moment constraints. All PDFs are generated using a 40 by 40 grid. By comparing these PDFs with the original PDA data of section 3 (Figures 3, 4 and 5), it is possible to assess the ability of the MEM to accurately reproduce these PDFs, and to highlight the importance of certain moment constraints for reproduction of particular features.

Figure 6 shows PDFs generated using MEM for position 1 in the DISI spray. The original PDA based PDFs (Figure 3(b)) exhibit distributions that to all intensive purposes are Gaussian in form. Comparison between the PDA and MEM PDFs would suggest that the PDFs can be reproduced reasonably well with just second order central moment constraints (mean and variance of ϕ, u_z, u_r). Figure 6(b) shows MEM PDFs generated with the addition of third order moment constraints and Figure 6(c) shows PDFs with the further addition of all covariances. These show minimal modification to the forms of the PDFs (third order and covariance moments negligible) and may be deemed unnecessary. In general the MEM PDFs tend to underestimate the peak values of each PDF. This is the behaviour one may expect given that the maximum entropy method generates PDFs of least statistical bias. It is interesting to note that the peak values tend to increase as additional moments are added. In Figure 6(c) the peaks are approximately 5-12% higher than in Figure 6(a). A quantitative analysis of the discrepancy in peak values between MEM and PDA is not useful in this situation due to the sensitivity of the PDA peaks to the mesh size used.

Figure 7 shows MEM PDFs for the second point in the DISI pressure swirl spray (edge of the spray cone). The PDA data (Figure 4) shows correlation between all three variables (ϕ, u_z, u_r), most significantly between u_z and u_r. It is clear from Figure 7(a) that these PDFs cannot be accurately reproduced with only mean and variance constraints. If the MEM is further constrained by covariances $\langle \phi u_z \rangle$, $\langle \phi u_r \rangle$ and $\langle u_z u_r \rangle$ these correlations are reproduced as shown in Figure 7(b). Figure 7(c) shows the effect of further addition of third order constraints but due to the symmetric nature of the original PDA data these constraints have negligible effect on the overall form of the MEM PDFs. Once again Figure 7 shows that as more constraints are added the MEM solver, the peak PDF values increase towards the PDA peak values.

Figure 6: MEM generated PDFs for the DISI pressure swirl spray position 1 ($z = 20mm$, $r = 0mm$). (i) Droplet size and axial velocity (ii) droplet size and radial velocity and (iii) axial velocity and radial velocity. Generated using moment constraints (a) to second order (b) to third order (c) to third order with covariances.

Figure 8 shows MEM generated PDFs for the steady charged spray (Figure 5). It is clear from Figure 8(a) that means and variances alone are not sufficient to reproduce the form of the PDFs at this position. Using just these constraints the MEM fails to reproduce the cross correlations and asymmetry features present in Figure 5. The Gauss like PDFs are far too 'diffuse' and peak values are an order of magnitude below those of the PDA PDFs. Addition of third order constraints (Figure 8(b)) allows the MEM to reproduce the off-centre peaks, however the PDFs still fail to represent the forms of the original PDA data. Further improvements are gained through the addition of covariance constraints, particularly for the $\phi - u_z$ PDF (Figure 8(ci)). Further improvements are obtained when the MEM is constrained by fourth order moments as shown in Figure 8(d).

5   CONCLUSION

Comparisons between real PDFs obtained from experimental PDA data and MEM reconstructions show that the MEM method is capable of reasonably accurate approximations of the multivariate PDFs given appropriate and sufficient constraints. Crudely the accuracy of the MEM method scales with the number and the order of the moment constraints. However under certain conditions good estimates can be obtained with relatively few low order constraints. For instance, as expected the MEM recovers Gaussian PDFs with only mean and variance input constraints. However, these MEM based PDFs tend to underestimate the peak values and it is necessary to further constrain the MEM to enhance accuracy of peak values. Where strong correlation exist between variables (e.g. u_z and u_r) it is necessary to include the covariance constraints to obtain an reasonable approximation to the original PDFs. Data showing asymmetry requires further constraint with third order constraints.

When considering the potential of the MEM in the context of a moment closure model for multiphase flow models,
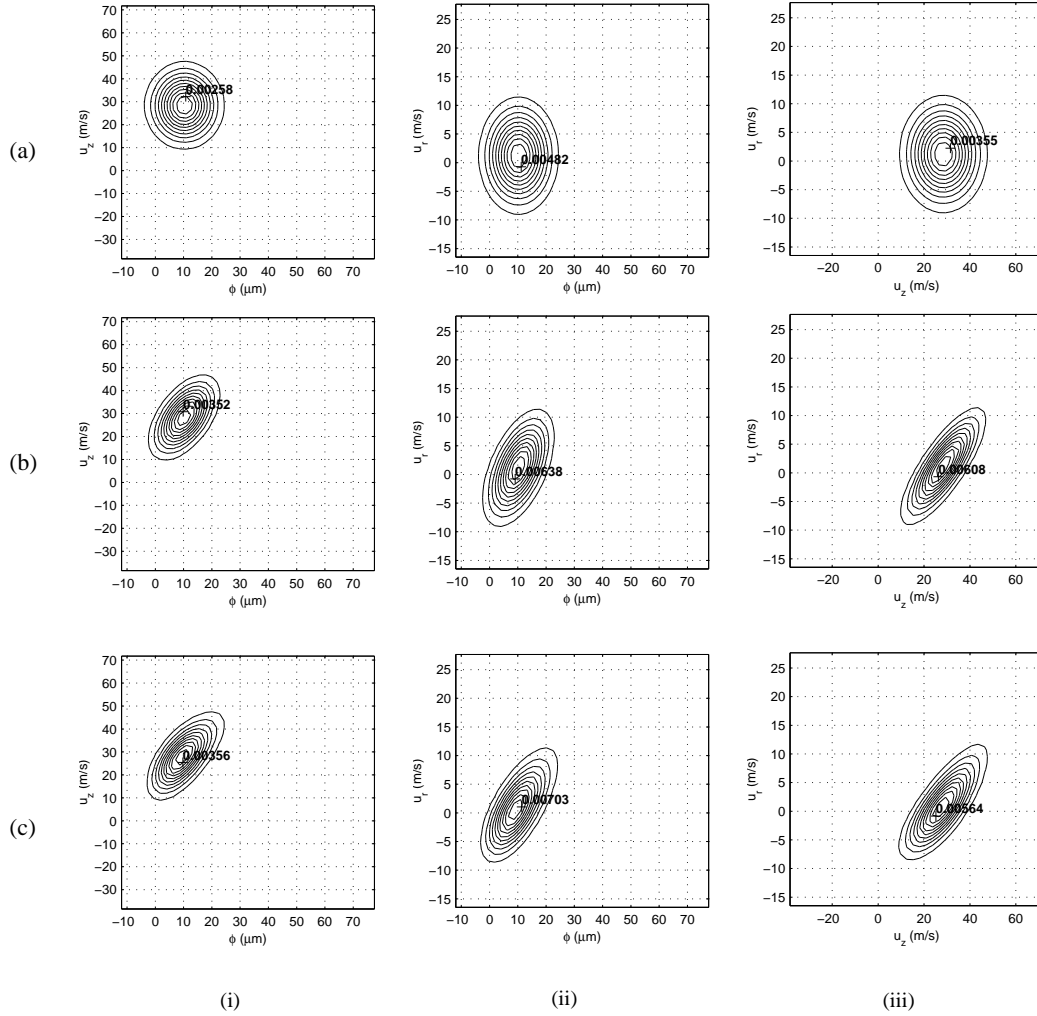
Figure 7: MEM generated PDFs for the DISI pressure swirl spray position 2 ($z = 20mm$, $r = 7.5mm$). (i) Droplet size and axial velocity (ii) droplet size and radial velocity and (iii) axial velocity and radial velocity. Generated using moment constraints (a) to second order (b) to second order plus covariances (c) to third order with covariances.

it must be realised the the suitability of the MEM is dependent on the nature of the flow. For simple isotropic flows a simple eddy viscosity model would provide sufficient information for constraint of the MEM and to allow the multiphase moment transport model to provide relatively accurate predictions relatively quickly. More complex flows exhibiting cross correlations and source terms that are not a function of transported moments require a more comprehensive set of constraints. Under these circumstances a model that transports second order moments of the multiphase fluid would appear more suitable. However, where there is mixture of 'ballistic' particles and 'diffusive' particles, even a second order moment transport model will fail to capture all of the physics.

NOMENCLATURE

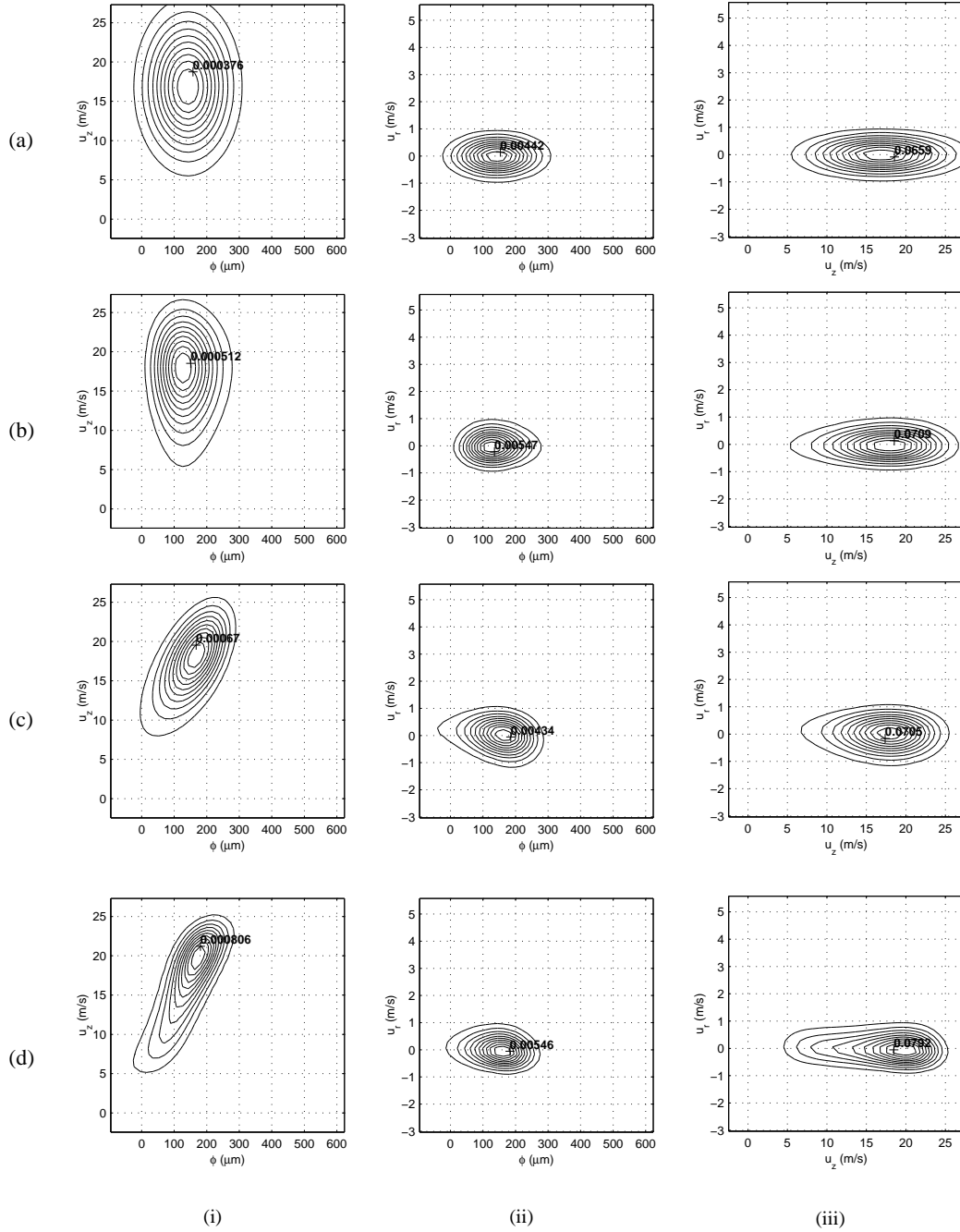|					
$\boldsymbol{U}_i$	i^{th} particle velocity	ms^{-1}	$\boldsymbol{u}$	Phase space velocity	ms^{-1}
$\boldsymbol{X}_i$	i^{th} particle position	m	$\boldsymbol{x}$	Phase space position	m
$\boldsymbol{\Phi}_i$	i^{th} particle diameter	m	ϕ	Phase space diameter	m
f	phase space density function	.	$\langle . \rangle$	Moment of PDF	.
S	Shannon entropy	.	u_z	Axial velocity	ms^{-1}
p	Probability density function	.	u_r	Radial velocity	ms^{-1}
N	Number of particles in dataset	.	N_b	Bins in phase space dimension	.

Figure 8: MEM generated PDFs for the steady charged spray ($z = 20mm$, $r = 0mm$). (i) Droplet size and axial velocity (ii) droplet size and radial velocity and (iii) axial velocity and radial velocity. Generated using moment constraints (a) to second order (b) to third order (c) to third order with covariances (d) to fourth order with covariances.

References

[1] A. A. Mostafa and H. C. Mongia. On the modelling of turbulent evaporating sprays: Eularian versus lagrangian approach. *Int. J. Heat Mass Trans.*, 30:2583–2593, 1987.

[2] M. W. Reeks. On a kinetic equation for the transport of particles in turbulent flows. *Phys. Fluids A*, 3:446–456, 1991.

[3] L. I. Zaichik. A statistical model of particle transport and heat transfer in turbulent shear flows. *Physics of Fluids*, 11:1521–1534, 1999.

[4] R. V. R. Pandya and F. Mashayek. Probability density function modelling of evaporating droplets dispersed in isotropic turbulence. *AIAA Journal*, 39:1909–1915, 2001.

[5] J. C. Beck. *Computational modelling of polydispersed sprays without segregation into droplet size classes*. PhD thesis, UMIST, 2000.

[6] A. J. White and M. J. Hounslow. Modelling droplet size distributions in polydispersed wet-steam flows. *Int. J. Heat Mass Transfer*, 43:1873–1884, 2000.

[7] M. R. Archambault. *A Maximum Entropy Moment Closure Approach to Modelling the Evolution of Spray Flows*. PhD thesis, Stanford, 1999.

[8] E. T. Jaynes. Information theory and statistical mechanics. *Phys. Review*, 106:620–630, 1957.

[9] C. E. Shannon. A mathematical theory of communication. *Bell Syst. Tech. J.*, 27:379–623, 1948.

[10] J. Paris and A. Vencovska. In defense of the maximum entropy inference process. *Int. J. Approx. Reasoning*, 17:77–103, 1997.

[11] R. W. Sellens. Prediction of the drop size and velocity distribution in a spray, based on the maximum entropy formalism. *Part. Part. Syst. Charact.*, 6:17–27, 1989.

[12] E. Babinsky and P. E. Sojka. Modelling drop size distributions. *Progress in Energy Combustion Science*, 28:303–329, 2002.

[13] K. Triballier, C. Dumouchel, and J. Cousin. Analysis of double-peak spray drop-size distribution from the application of the maximum entropy formalism. In *ICLASS 2004*, 2003.

[14] E. V. Volpe. *Closure relations as determined by the maximum entropy method and near equilibrium conditions*. PhD thesis, Stanford, 2000.

[15] G. Wigley. Presentation - some data with regard to imaging and pda studies of the mitsubishi gdi injector spraying at 50 bar gasoline pressure into air under atmospheric conditions. 2004.

[16] J. S. Shrimpton and A. J. Yule. Characterisation of charged hydrocarbon sprays for application in combustion systems. *Experiments in Fluids*, 26:460–469, 1999.

[17] Y. Alhassid, N. Agmon, and R. D. Levine. An upper bound for the entropy and its applications to the maximal entropy problem. *Chemical Physics Letters*, 53:22–26, 1978.

[18] J. C. Lagarias, J. A. Reeds, M. H. Wright, and P. E. Wright. Convergence properties of the nelder-mead simplex method in low dimensions. *SIAM Journal of Optimization*, 9:112–147, 1998.